

---

# Watching Too Much Television is Good: Self-Supervised Audio-Visual Representation Learning from Movies and TV Shows

---

Anonymous Author(s)

Affiliation

Address

email

## Abstract

1 The abundance and ease of utilizing sound, along with the fact that auditory clues  
2 reveal so much about what happens in the scene, make the audio-visual space a  
3 perfectly intuitive choice for self-supervised representation learning. However,  
4 the current literature suggests that training on *uncurated* data yields considerably  
5 poorer representations compared to the *curated* alternatives collected in supervised  
6 manner, and the gap only narrows when the volume of data significantly increases.  
7 Furthermore, the quality of learned representations is known to be heavily influ-  
8 enced by the size and taxonomy of the curated datasets used for self-supervised  
9 training. This begs the question of whether we are celebrating too early on catching  
10 up with supervised learning when our self-supervised efforts still rely almost exclu-  
11 sively on curated data. In this paper, we study the efficacy of learning from Movies  
12 and TV Shows as forms of uncurated data for audio-visual self-supervised learning.  
13 We demonstrate that a simple model based on contrastive learning, trained on a  
14 collection of movies and TV shows, not only dramatically outperforms more com-  
15 plex methods which are trained on orders of magnitudes larger uncurated datasets,  
16 but also performs very competitively with the state-of-the-art that learns from  
17 large-scale curated data. We identify that audiovisual patterns like the appearance  
18 of the main character or prominent scenes and mise-en-scène which frequently  
19 occur through the whole duration of a movie, lead to an overabundance of easy  
20 negative instances in the contrastive learning formulation. Capitalizing on such  
21 observation, we propose a hierarchical sampling policy, which despite its simplicity,  
22 effectively improves the performance, particularly when learning from TV shows  
23 which naturally face less semantic diversity.

## 24 1 Introduction

25 Recently, there has been tremendous progress in self-supervised learning from still images, where the  
26 standard supervised training has been outperformed in a variety of image-related tasks [7, 8, 15, 29].  
27 The appeal of detaching representation learning from human annotations is rooted not only in the  
28 non-trivial challenges of scaling-up the labeling process, but also in the ill-defined task of determining  
29 a proper taxonomy with generalization power and transferability. Both challenges only exacerbate as  
30 we move from images to videos, where the notion of time is involved and the complexity of visual  
31 concepts increases. Simply considering the number of training instances or even the cardinality of  
32 the label set is not sufficient to conclude if one large-scale supervised dataset is more suitable than  
33 another for transfer learning in video classification tasks [20]. That is, the abundance of attention  
34 which video self-supervised learning has lately received is only to be expected. While many research  
35 efforts in this area extend the contributions made initially in the image domain to the video domain,

36 others, including our work, have explored harnessing additional modalities such as audio or text for  
37 multi-modal self-supervised learning [2, 3, 4, 22, 27, 31, 37, 36, 39].

38 From the current state-of-the-art one makes two major conclusions. First, the quality of learned  
39 representations, evaluated by fine-tuning on downstream tasks, is heavily influenced by the size and  
40 taxonomy of the pretraining datasets [2, 3, 39]. Second, an *uncurated* pretraining dataset yields  
41 considerably poorer representations compared to a *curated* one and the gap only narrows when the  
42 total amount of pretraining data significantly increases [3]. Curated data refers to likes of *supervised*  
43 large-scale action recognition and audio classification datasets such as Kinetics [6], IG-Kinetics  
44 [12], AudioSet [11], and YouTube-8M [1]. While the human-annotated labels are not accessed for  
45 self-supervised pretraining, videos being trimmed and from a label set of limited cardinality with  
46 biased sampling distribution<sup>1</sup> implicitly acts as a sort of supervision. On the other hand, an *uncurated*  
47 data refers to likes of IG-Random[3], simply a body of unlabeled videos collected blindly with  
48 none of the aforementioned careful human-involvements. That being said, we know that something  
49 as simple as having access to a clean object-centric training data, like Imagenet, can be indirectly  
50 exploited by contrastive self-supervised learning in image domain to obtain additional performance  
51 gain [41] on the downstream tasks which exhibit similar properties. The analogous to it of course are  
52 the well trimmed closed-set curated datasets which are being extensively used in the literature for  
53 video self-supervised pretraining, while downstream evaluations focus on benchmarks with similar  
54 characteristics. Our work aims at comprehensively exploring the efficacy of learning from Movies  
55 and TV Shows, as forms of uncurated data, for audio-visual self-supervised learning.

56 Many of us can relate to an experience in movie theaters when the sound of the engine, first perceived  
57 by our left ear, is gradually heard more by the right ear as a car moves from the left side of the  
58 screen to the right side. Another example is a scene in which an object, like a helicopter, approaches  
59 the camera from distance and eventually flies over it. In this case, the perceived sound not only  
60 changes in loudness but also transitions from front to back, in concert with the visuals, giving the  
61 audience a more realistic feeling as if they are indeed positioned behind the camera. Besides, with  
62 art being inherently novel, two movies even if they share genres or revolve around similar story  
63 lines often deliver quite different experiences and portray distinct visuals, thanks to the extremely  
64 artist-driven creative process behind such productions. We hypothesize that the aforementioned high  
65 audio fidelity, and inherent semantic diversity characterize long-form content<sup>2</sup> as potentially a very  
66 rich source for self-supervised multi-modal representation learning. It is worth emphasizing that in  
67 spirit of uncurated data, we not only blindly sample from a large collection of movies and TV shows  
68 when constructing our pretraining dataset, but also perform ablation studies on the effect of genre  
69 distribution, the closest we have to taxonomy in the curated datasets, confirming that the quality of  
70 learned representations is agnostic with respect to such statistics.

71 To the best of our knowledge, we are the first to solely rely on uncurated data and study the efficacy of  
72 self-supervised multi-modal representation learning from movies and TV shows. Despite meaningful  
73 domain gap between our pretraining data and the space of downstream tasks, we obtain representations  
74 which are very competitive with those learned from curated datasets. This is particularly important as  
75 we follow a much simpler modeling approach in comparison with the state-of-the art.

## 76 2 Related Work

77 Self-supervised learning techniques define *pretext* tasks, mostly inspired by the natural structures  
78 in the data, in order to generate supervisory signals for training. Despite the plethora of proposed  
79 *pretext* tasks in the literature, these approaches can be coarsely divided into two groups, namely  
80 *pretext learning*, and *pretext-invariant* methods. Approaches which fall in the former bucket, usually  
81 apply a form of transform, randomly drawn from a parametric family, to the input data then optimize  
82 for predicting the parameters of the chosen transformation. Predicting the relative position of image  
83 patches [9], solving jigsaw puzzles [33], estimating artificial rotations [13], colorization [50], context  
84 encoders learned through inpainting [38], and learning by counting scale and split invariant visual  
85 primitives [34], are among many methods which belong to this category. Similar techniques have  
86 been extended from images to videos [10, 21, 24, 25, 30, 46, 48, 49], where in addition to the  
87 spatial context, the temporal domain, and the arrow of time have been heavily exploited. In contrast,

---

<sup>1</sup>the associated taxonomy has similarities with those of downstream benchmarks [3]

<sup>2</sup>alternatively referring to movies and TV shows

88 *pretext-invariant* methods [5, 7, 8, 15, 18, 17, 29, 35, 39, 44] are built on the concept of maximizing  
 89 mutual information across augmented versions of a single instance, and are mostly formulated as  
 90 contrastive learning. In other words, a pretext is used to generate different views of a single input  
 91 for which the learning algorithm aims to maximize the intra-instance similarity, across variety of  
 92 transformations. Our work falls within this category, however we function in a multi-modal realm  
 93 employing both audio and video.

94 Earlier works which harnessed audio and video for representation learning, have leveraged audio-  
 95 visual temporal synchronization [22, 36], correspondence [4], and cross-modal clustering [3, 37]. The  
 96 work by Patrick *et al.* [39] proposes a generalized data transformation in order to unify a variety of  
 97 audio-visual self-supervised pretext tasks through a noise contrastive formulation. This work is close  
 98 to ours in choice of objective function and data type, yet we employ no augmentation (except *modality*  
 99 *projection* in the terminology of [39]), and solely focus on capitalizing the advantages of learning  
 100 from long-form content. Morgado *et al.* [31] show that cross-modal discrimination is important for  
 101 learning good audio and video representations, something which was also pointed out earlier in a  
 102 clustering framework [3]. Beyond that, [31] generalizes the notion of instance-level positive and  
 103 negative examples by exploring cross-modal agreement where multiple instances are grouped together  
 104 as positives by measuring their similarity in both the video and audio feature spaces. While we also  
 105 adopt a cross-modal noise contrastive estimation loss, we stick with the vanilla version, instance-level  
 106 positive and negatives, and do not use any memory bank feature representations. Finally, Alayrac *et*  
 107 *al.* [2] recently proposed a multi-modal versatile network capable of simultaneously learning from  
 108 audio, video and text. Building on the intuition that different modalities are of different semantic  
 109 granularity, audio and video are first compared in a fine-grained space while text is compared with  
 110 the aforementioned modalities in a lower dimensional coarse-grained space. In our experiments, we  
 111 compare with a variant of [2] where only audio and video modalities are utilized.

### 112 3 Approach

113 **Notations and Architecture.** Our pretraining dataset is denoted by  $\mathcal{X} = \{\mathcal{X}_n | n \in [1 \dots N]\}$ ,  
 114 where  $\mathcal{X}_n = \{x_{n,m} | m \in [1 \dots M_n]\}$  contains  $M_n$  non-overlapping audiovisual snippets which are  
 115 temporally segmented from the duration of the  $n^{\text{th}}$  long-form content in the dataset. Each snippet  
 116 includes both audio and video modalities, formally  $x_{n,m} = (a_{n,m}, v_{n,m})$ , where  $a_{n,m} \in \mathbb{R}^{1 \times P \times Q}$   
 117 and  $v_{n,m} \in \mathbb{R}^{3 \times T \times H \times W}$ .  $T$ ,  $H$ , and  $W$  denote the number of frames, height and width of the video,  
 118 while  $P$ , and  $Q$  respectively stand for the number of mel filters, and audio frames. Video and audio are  
 119 processed through 18-layers deep R(2+1)D [45] and ResNet [16] architectures, respectively referred  
 120 to as  $f: \mathbb{R}^3 \rightarrow \mathbb{R}^{d_f}$  and  $g: \mathbb{R}^1 \rightarrow \mathbb{R}^{d_g}$ . Inspired by [7], we use *projection heads*,  $h_f: \mathbb{R}^{d_f} \rightarrow \mathbb{R}^d$  and  
 121  $h_g: \mathbb{R}^{d_g} \rightarrow \mathbb{R}^d$ , to map corresponding representations into a common  $d$ -dimensional space before  
 122 computing the contrastive loss. The shallow architecture of  $h_f$  and  $h_g$  consists of two convolution  
 123 layers, separated by Batch Normalization [19] and ReLU [32], followed by global average pooling.  
 124 Once self-supervised pretraining finished, we discard the projection heads and fine-tune  $f$  and  $g$  for  
 125 respective downstream tasks.

126 **Loss Function.** With a slight abuse of notation<sup>3</sup>,  $\mathcal{B} = \{x_i = (a_i, v_i) | i \in [1 \dots B]\}$  represents a  
 127 minibatch of size  $B$ , where video and audio modalities associated with the  $i^{\text{th}}$  sample,  $x_i$ , are denoted  
 128 by  $v_i$  and  $a_i$ . We use  $z_v^i = h_f(f(v_i))$  and  $z_a^i = h_g(g(a_i))$  to represent the associated embeddings  
 129 generated by projection heads, and optimize the noise-contrastive loss [14] shown in 1 in order  
 130 to maximize the symmetric joint probability between audio and video. For the  $i^{\text{th}}$  element in the  
 131 minibatch,  $(z_v^i, z_a^i)$  serves as the positive pair, while assuming negative pairs for both modalities,  
 132  $\mathcal{N}_i = \{(z_v^i, z_a^j), (z_v^j, z_a^i) | j \in [1 \dots B], i \neq j\}$  constitutes the set of negative pairs.

$$\mathcal{L} = - \sum_{i=1}^B \log \left( \frac{e^{(z_v^i)^\top (z_a^i)}}{e^{(z_v^i)^\top (z_a^i)} + \sum_{(z'_v, z'_a) \in \mathcal{N}_i} e^{(z'_v)^\top (z'_a)}} \right) \quad (1)$$

133 Most of the previous works [2, 31, 39] normalize the embeddings before computing the contrastive  
 134 loss and employ a temperature hyper-parameter, often denoted by  $\tau$  as in [2, 31], to control the

<sup>3</sup> $i$  enumerates elements in the minibatch

135 smoothness for the distribution of pairwise similarities. In contrast, we have chosen to operate in an  
 136 unnormalized embedding space. Besides the obvious benefit of eliminating the need for tuning  $\tau$ , we  
 137 empirically show that such decision does not affect the quality of the learned representations.

138 **Sampling Policy.** Contrastive loss function shown in Equation 1 is computed over  $B$  training  
 139 instances, each in form of an audiovisual snippet. A naive sampling policy may ignore the fact that  
 140 snippets comprising the pretraining dataset are in fact temporal segments that were trimmed from  
 141 longer-form contents, *i.e.* movies and TV shows. Such an assumption treats our training data as  
 142 independent and identically distributed random variables from  $\bigcup_{n=1}^N \mathcal{X}_n$ , which constitutes the default  
 143 sampling policy that is commonly used in the general deep learning literature. However, in reality,  
 144 commonalities and correlations do exist along the temporal axis of a movie or TV show, things like  
 145 audio mastering artifacts, frequent appearance of the main character’s face and voice, thematic music,  
 146 repetitive scenes and *mise-en-scène*<sup>4</sup>, all of which contribute to breaking the previously discussed  
 147 i.i.d assumption. This is even more pronounced when we deal with multiple episodes of the same TV  
 148 show appearing in the pretraining dataset<sup>5</sup>. Note that, sampling from no video data is going to be i.i.d  
 149 but in this case the temporal correlations extend for much longer given our entities are movies and TV  
 150 shows. Thus, it is more accurate to think of  $\mathcal{X}$  having multiple underlying domains, oriented towards  
 151 exclusive properties which different long-form contents are characterized by. We hypothesize that  
 152 during training, model gradually discovers such patterns of commonalities, which are not semantically  
 153 valuable, and latches onto those to quickly minimize Equation 1 leading to poor generalization<sup>6</sup>. The  
 154 reason being  $B \ll N$ , hence for  $n \sim \mathbb{U}(1, N)$  and  $m \neq m'$ ,  $P(x_{n,m} \in \mathcal{B} \wedge x_{n,m'} \in \mathcal{B})$  is negligible.  
 155 In other words, the set of negative pairs in Equation 1 mainly includes pairs for which audio and  
 156 video come from two different movies or TV shows, thus due to the aforementioned artifacts behave  
 157 as easy negatives.

158 In order to quantitatively measure our hypothesis, we define different distributions, shown in Equation  
 159 2, over the space of audio-visual similarity.  $\mathcal{S}^+$  indicates the space of correct matches, *i.e.* where  
 160 audio and video correspond to the same snippet.  $\mathcal{S}^-$  indicates the space where audio and video do  
 161 not correspond yet belong to the same movie or TV show. Finally,  $\mathcal{S}^\neq$  indicates the space in which  
 162 audio and video are sampled from two distinct long-form content, hence naturally do not correspond.

$$(z_v^{n,m})^\top (z_a^{n',m'}) \sim \begin{cases} \mathcal{S}^+, & \text{if } n = n' \wedge m = m' \\ \mathcal{S}^-, & \text{if } n = n' \wedge m \neq m' \\ \mathcal{S}^\neq, & \text{if } n \neq n' \wedge \forall(m, m') \end{cases} \quad (2)$$

163 With that, and KL denoting Kullback–Leibler divergence,  $\text{KL}(\mathcal{S}^- \parallel \mathcal{S}^+)$  measures the expected  
 164 difference between positive and negative pairs within the same movie or TV show. Ideally, this should  
 165 increase as the training progresses, since the model gradually learns audio-video correspondence by  
 166 minimizing Equation 1. Meanwhile, the i.i.d assumption suggests  $\text{KL}(\mathcal{S}^- \parallel \mathcal{S}^+) \simeq \text{KL}(\mathcal{S}^\neq \parallel \mathcal{S}^+)$   
 167 and  $\text{KL}(\mathcal{S}^- \parallel \mathcal{S}^\neq) \simeq 0$ , yet as we empirically illustrate later,  $\text{KL}(\mathcal{S}^- \parallel \mathcal{S}^+) < \text{KL}(\mathcal{S}^\neq \parallel \mathcal{S}^+)$  and  
 168  $\text{KL}(\mathcal{S}^- \parallel \mathcal{S}^\neq)$  is rather large, indicating that, upon convergence and on a held-out set, model has  
 169 a harder time pushing apart negative pairs when audio and video come from the same underlying  
 170 long-form content. Next, we explain how a simple alternative policy which samples  $k$  snippets  
 171 from each long-form content effectively reduces both of the *discrepancy measures*, referring to  
 172  $\text{KL}(\mathcal{S}^- \parallel \mathcal{S}^\neq)$  and  $\text{KL}(\mathcal{S}^\neq \parallel \mathcal{S}^+) - \text{KL}(\mathcal{S}^- \parallel \mathcal{S}^+)$ , while yielding better generalization on a range  
 173 of downstream tasks.

174 To ameliorate the aforementioned optimization challenge, we take a hierarchical approach. In  
 175 particular, we first uniformly sample a long-form content,  $n \sim \mathbb{U}(1, N)$ , and then draw  $k$  distinct  
 176 snippets from  $\mathcal{X}_n$ , creating  $\{x_{n,m} | m \in \mathcal{M}_n\}$ , where  $\mathcal{M}_n \subset [1 \cdots M_n]$  and  $|\mathcal{M}_n| = k$ . This ensures  
 177 that for  $x_i \in \mathcal{B}$ ,  $\mathcal{N}_i$  always includes  $2k - 2$  pairs sampled from the same movie or TV show to  
 178 which  $x_i$  belongs. By putting constraints on  $\mathcal{M}_n$ , specifically how temporally far from each other  
 179 the  $k$  samples are drawn, we may go one step further and to some extent control the audiovisual  
 180 similarity between snippets. This serves as an additional knob to tune for hard negative sampling.  
 181 The intuition is that, the larger narrative of a professionally made movie or TV show is composed of  
 182 shorter units called *scene*. Each scene comprises a complete event, action, or block of storytelling and

<sup>4</sup>collectively referred to as *content-exclusive artifacts*

<sup>5</sup>alternatively think of it as a very long movie created by stitching different episodes together

<sup>6</sup>refer to supplemental material for illustrations of training loss

183 normally takes place in one location and deals with one action. That is, if our samples are temporally  
184 close, it is more likely for corresponding snippets to be highly correlated and/or look/sound alike.  
185  $k \leq \max[\mathcal{M}_n] - \min[\mathcal{M}_n] + 1 \leq w \leq M_n$  defines the bounds on our sampling policy, where  $w$ ,  
186 standing for a sampling *window*, determines the farthest two out of  $k$  samples drawn from  $\mathcal{X}_n$  can  
187 be. Accordingly,  $w = k$  represents the case where all  $k$  samples are temporally adjacent, hence  
188 the expected audiovisual similarity is maximized due to temporal continuity in content. We show  
189 that having such level of hard negatives, even with a small  $k$ , prevents proper training and results in  
190 performance degradation. On the other hand,  $w = M_n$  indicates random sampling where no temporal  
191 constraint is imposed on  $\mathcal{M}_n$ , thus samples are less likely to be drawn from adjacent time-stamps.  
192 In this case, expected audiovisual similarity (*i.e.* hardness of negative pairs) is mainly derived from  
193 global content-exclusive artifacts like, color palette, frequent appearance of the main character’s face  
194 and voice, repetitive scenes, and etc. The rest of the spectrum provides middle grounds where two  
195 samples drawn from  $\mathcal{X}_n$  can at most be  $w + 1$  snippets apart, something reminiscent of temporal  
196 locality. Our sampling policy can be easily implemented in a few lines of Python. Please refer to  
197 supplemental material for further details.

## 198 4 Experiments

### 199 4.1 Experimental Setup

200 **Datasets and Reproducibility.** We use full-length movies and episodes of TV shows for self-  
201 supervised pretraining. Titles are randomly chosen from a large collection spanning over a variety of  
202 genres, namely Drama, Comedy, Action, Horror, Thriller, Sci-Fi and Romance. All audio is in English  
203 language. Our Movie dataset, consists of 3.6K films with an average duration of 105 minutes. Our TV  
204 dataset includes 9.2K episodes from a total of 581 shows with an average duration of 42 minutes per  
205 episode. Each of our datasets comprises 0.7 years worth of uncurated audiovisual content, which is  
206 significantly smaller than IG-Random [3] with variants at 5 and 21 years. Scaling up our pretraining  
207 datasets to volumes comparable to the IG-Random [3] while possible is non-trivial and demands  
208 dramatically larger compute resources for training, something which we currently cannot afford.  
209 Given that we cannot publicly release our dataset due to copyright reasons, we acknowledge that it is  
210 not possible for other research groups to fully reproduce our results. However, we intend to make  
211 available the pretrained models and hope that research community finds them, along with the other  
212 contributions of this work, of value whether within the context of self-supervised learning or adoption  
213 for various downstream tasks. We would like to emphasize that similar limitations have precedents  
214 in multiple earlier works including but not limited to [3, 12, 26, 43]. To evaluate the efficacy of  
215 self-supervised audio-visual representation learning from movies and TV shows, we follow recent  
216 works [3, 39, 31, 2] and benchmark UCF101[42] and HMDB51[23] for action recognition, along  
217 with ESC50[40] for audio classification. Results for the ablation studies are reported on the split-1 of  
218 the corresponding datasets. Following the standard protocol, we report the average performance over  
219 all splits when we are comparing with the state-of-the-art.

220 **Pretraining.** Unless mentioned otherwise, we use video snippets with 16 frames at 5 fps. For data  
221 augmentation, we resize the shorter side to 190 pixels, then randomly crop them into  $158 \times 158$  pixels.  
222 As for sound, we compute mel spectrogram from the raw audio at 48K sample rate using 96 mel  
223 filters and an FFT window of 2048, while the number of samples between successive frames is set to  
224 512. For data augmentation, we randomly drop out up to 25% from either temporal or frequency axis  
225 of the 2-D mel spectrogram image. Training uses a batch size of 512 and takes on average 42 hours  
226 on 8 NVIDIA A100 GPUs. The dimension of audio-video joint embedding space,  $d$ , is set to 512.

227 **Downstream Evaluation.** For training on UCF101 [42] and HMDB51 [23], we use video clips that  
228 are 32 frames long at 10 fps. Unless mentioned otherwise, these clips are randomly chosen from the  
229 duration of the video instances. A scale jittering range of [181, 226] pixels is used and we randomly  
230 crop the video into  $158 \times 158$  pixels. Furthermore, random horizontal flipping and color jittering  
231 are employed. During inference, 10 temporal clips are uniformly sampled where each is spatially  
232 cropped in 3 ways (left, center, right) resulting in a total of 30 views. We then average the model  
233 predictions across these 30 views and report top-1 classification accuracy. For training on ESC50  
234 [40], we use 3-seconds clips which are randomly chosen from the duration of the audio instances  
235 and apply time and frequency masking to spectrogram images for data augmentation. The maximum  
236 possible length of the mask is 50% of the corresponding axis. We do not use any scale jittering or  
237 random cropping on the spectrograms. During inference, 10 temporal clips are uniformly sampled

238 and we average the model predictions across these 10 views and report top-1 classification accuracy.  
 239 For further implementation details, please refer to the supplemental material.

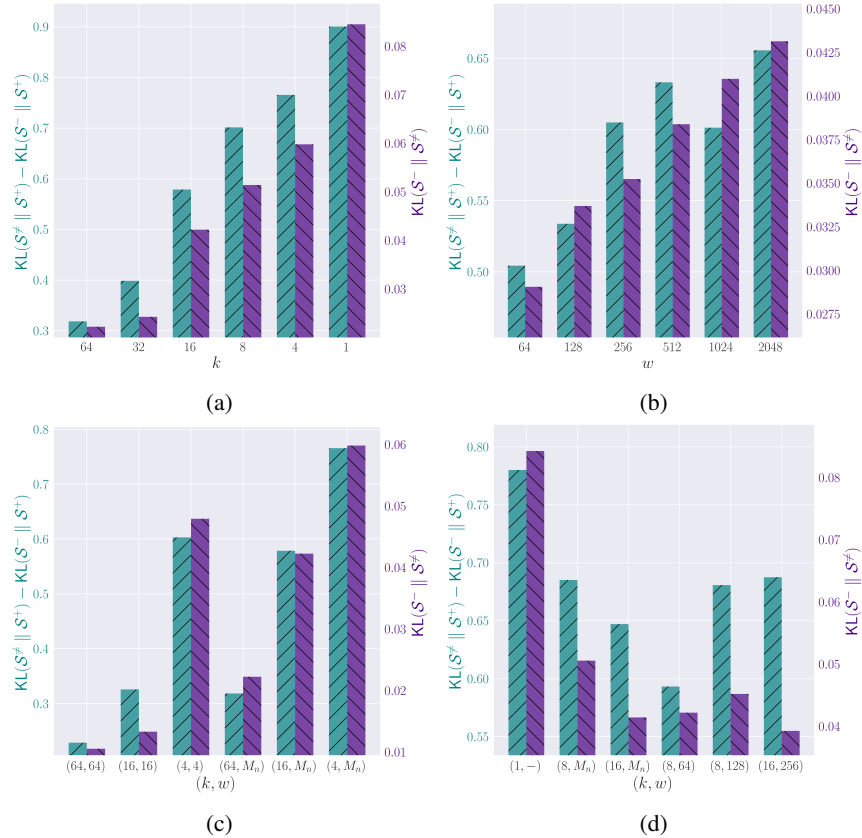


Figure 1: Ablation study of the proposed sampling policy on reducing the discrepancy measures.

## 240 4.2 Ablation Study

241 In the following, we discuss multiple ablation studies to  
 242 assess our main hypothesis that, a hierarchical sampling  
 243 policy, as described in Section 3, enables better repre-  
 244 sentations to be learned by increasing the portion of hard  
 245 negative pairs which the contrastive loss function observes.  
 246 Here, pretraining uses 90% of either Movie or TV dataset,  
 247 while the remaining 10% constitute a held-out validation  
 248 set<sup>7</sup> on which we report the discrepancy measures.

249 **Sample size ( $k$ )** Figure 1a illustrates that compared to  
 250 the baseline sampling denoted by  $k = 1$ , our approach  
 251 ( $k > 1$ ) effectively shrinks the gap between  $S^-$  and  $S^+$   
 252 when measured either directly or against  $S^+$ . Its pattern  
 253 of behavior also perfectly follows our earlier intuition (ref.  
 254 Section 3). In particular, given a fixed minibatch budget,  
 255 a larger  $k$  favors more training instances to be sampled  
 256 from fewer number of long-form contents. That increases  
 257 the portion of hard negative pairs, thus pushes the con-  
 258 trastive loss to more aggressively separate mismatched  
 259 audio-video pairs from the same movie, which leads model  
 260 to maintain less of the content-exclusive artifacts in the embedding space. In the most extreme case,  $k = 64$ , all the training instances are

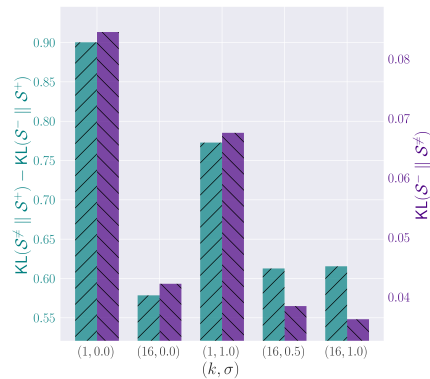


Figure 2: Effect of color jitter on the discrepancy measures.

<sup>7</sup>Given a TV show, either all or none of its episodes are included in the held-out set.

261 sampled from the same movie. From Table 1, we observe that different variants of our sampling  
 262 policy, with no imposed temporal constraint, *i.e.*  $w = M_n$ , outperform the baseline on all three  
 263 downstream tasks

264 **Sampling window ( $w$ )** Smaller  $w$  forces samples  
 265 that belong to same movie to be drawn from a shorter  
 266 temporal window, hence growing the probability that  
 267 they look/sound very much alike (*i.e.* harder neg-  
 268 ative pairs). That is, it should further diminish the  
 269 discrepancy measures. Figure 1b illustrates this be-  
 270 havior where we gradually increase  $w$  while  $k = 16$ .  
 271 However, from Table 1, it does not seem that tuning  
 272 for  $w$ , *i.e.*  $w \neq M_n$ , provides a meaningful gain on  
 273 downstream tasks. This implies that commonalities  
 274 which persist throughout the duration of a movie are  
 275 sufficiently powerful signals to be exploited for gener-  
 276 ating hard negatives. We hypothesize that different  
 277 *scenes* both within and across different movies and  
 278 TV shows are of variety of length, thus a fixed  $w$   
 279 is sub-optimal. Ideally, we should identify scene  
 280 boundaries and dynamically modify  $w$  during  
 281 sampling, something which we leave for future iter-  
 282 ations of this work.

283 **Temporally adjacent samples.** Along the lines  
 284 of previous observations, Figure 1c shows that in-  
 285 deed drawing temporally adjacent snippets from  
 286 the same long-form content, *i.e.*  $w = k$ , results  
 287 in aggressively reducing the discrepancy measures.  
 288 This behavior is agnostic with respect to  $k$  yet ex-  
 289 acerbates as  $k$  grows. Note that, the contrastive  
 290 loss is an instance-discrimination objective func-  
 291 tion. Therefore, forcing it to distinguish between  
 292 temporally adjacent snippets, that naturally sound  
 293 and look extremely similar, leaves no choice for  
 294 the model but to discard valuable semantic notions,  
 295 which predictably leads to poor representations, also  
 296 confirmed by result reported in Table 1.

297 **Movies vs. TV Shows.** To confirm that our sampling policy behaves consistently across both movies  
 298 and TV shows, Figure 1d illustrates the discrepancy measures computed on TV dataset. We observe  
 299 similar effectiveness when using  $k$  and  $w$  as tuning knobs for reducing either  $\text{KL}(S^- \parallel S^\neq)$  or the  
 300 gap between  $\text{KL}(S^- \parallel S^+)$  and  $\text{KL}(S^\neq \parallel S^+)$ . Table 1 demonstrates that different variants of our  
 301 approach significantly outperform the baseline, *i.e.*  $k = 1$ . We attribute the larger gains achieved  
 302 when using TV instead of Movie dataset to the fact that content diversity is naturally lower when  
 303 pretraining on TV shows since each one includes many episodes that all are characterized with the  
 304 same content-exclusive artifacts.

305 **Color jitter.** We have established so far that commonalities which persist throughout the duration  
 306 of a long-form content, things likely associated with color pallet, frequent appearance of the main  
 307 character’s face and voice, and repetitive scenes can be exploited for learning better representations.  
 308 That is, one may naturally assume that employing data augmentation techniques like color jitter  
 309 should be helpful since by distorting content-exclusive visual artifacts, color jitter is expected to  
 310 reduce  $\text{KL}(S^- \parallel S^\neq)$ . Figure 2 illustrates the effect of color jitter, where brightness, contrast, and  
 311 saturation jitter values are chosen uniformly from  $[\max(0, 1 - \sigma), 1 + \sigma]$ . We observe that color  
 312 jitter reduces the discrepancy measures for the baseline but not as much as it can be obtained by our  
 313 proposed sampling policy ( $k > 1$ ), and even then according to Table 2 only yields a slight gain on  
 314 downstream tasks.

315  **$\ell_2$ -normalized feature space.** The common practice [2, 31, 39, 7] is to compute contrastive loss in  
 316 an  $\ell_2$ -normalized feature space, where according to [47] the temperature hyper-parameter,  $\tau$ , controls

Table 1: Ablation study of the proposed sampling policy on different downstream tasks, measured by top-1 classification accuracy.

pretraining dataset: Movie				
$k$	$w$	HMDB51	ESC50	UCF101
1	-	60.32	86.50	85.69
4	$M_n$	61.37	89.91	85.38
8	$M_n$	62.09	88.75	86.06
16	$M_n$	62.92	88.33	86.30
32	$M_n$	61.04	88.00	85.98
64	$M_n$	61.30	86.83	85.43
16	64	60.26	87.00	83.61
16	128	60.58	86.50	85.30
16	256	62.02	87.75	84.85
16	512	61.30	87.08	85.38
16	1024	60.65	86.16	84.61
16	2048	61.83	87.66	85.11
4	4	60.19	88.00	84.66
16	16	56.86	88.75	82.71
64	64	57.45	84.58	82.68
pretraining dataset: TV				
$k$	$w$	HMDB51	ESC50	UCF101
1	-	56.40	85.50	84.37
8	$M_n$	61.50	87.50	85.96
16	$M_n$	61.69	89.00	85.64
8	64	60.58	88.00	85.96
8	128	60.00	85.66	85.77
16	256	61.30	86.41	85.01

Table 4: Effect of self-supervised learning from curated versus uncurated data on different downstream tasks. The “years” column indicates the duration of the pretraining datasets in years.

method	pretraining dataset	uncurated	years	HMDB51	ESC50	UCF101
Ours	Movie	✓	0.7	62.9	88.3	86.3
Ours	TV	✓	0.7	61.7	89.0	85.6
XDC[3]	IG-Random16M	✓	5	55.2	84.3	84.1
XDC[3]	IG-Random65M	✓	21	61.2	86.3	88.8
XDC[3]	IG-Kinetics16M	✗	5	57.3	82.5	87.6
XDC[3]	IG-Kinetics65M	✗	21	63.1	84.8	91.5

317 the strength of penalties on hard negative samples. We explored this with two widely-used  $\tau$  values.  
 318 From Table 2, we observe that compared to operating in an unnormalized embedding space, adopting  
 319 such design choice results in a large performance drop on HMDB51[23] while other downstream  
 320 benchmarks see only negligible gains.

321 **Curated vs. Uncurated data.** To the best of  
 322 our knowledge, the only other uncurated dataset  
 323 used for audio-visual self-supervised learning is IG-  
 324 Random[3]<sup>8</sup>. Table 4 confirms that learning from un-  
 325 curated movies and TV shows is extremely effective.  
 326 Our results significantly exceed those of XDC[3]  
 327 obtained on IG-Random16M despite using a sim-  
 328 pler model and 7 times smaller volume of pretrain-  
 329 ing data. Even in comparison to IG-Random65M  
 330 with 30 times larger data, we obtain better perfor-  
 331 mances on 2 out of 3 benchmarks. The most promis-  
 332 ing of our findings though is how competitive our  
 333 results are against XDC[3] when it is trained on  
 334 variants of IG-Kinetics which are not only curated  
 335 but also orders of magnitude larger. With all that,  
 336 we confidently reject the notion that audio-visual  
 337 self-supervised learning from uncurated data con-  
 338 siderably lags behind utilizing large-scale curated  
 339 datasets.

340 **Effect of genre.** The distribution of genre among  
 341 movies used in our pretraining is the closest we  
 342 have to taxonomy in the curated datasets. So, it is  
 343 worth examining the quality of our learned repre-  
 344 sentations under various genre distributions. To do  
 345 so, given a fixed pretraining budget ( $N = 1.6K$ ), we  
 346 compare four different scenarios where movies used  
 347 in the pretraining are distributed i) non-uniformly  
 348 over all genres except Drama, and Comedies, ii)  
 349 non-uniformly over Drama, and Comedies, iii) uni-  
 350 formly over all genres, and iv) non-uniformly over  
 351 all genres. Table 3 confirms that indeed there is very little difference between the aforementioned  
 352 setups when it comes to transfer learning to the downstream tasks.

### 353 4.3 Comparison with state-of-the-art

354 Table 5 compares our proposed approach of learning from Movies and TV shows against the best  
 355 performing audio-visual self-supervised learning methods. In general, our numbers are comparable  
 356 with the best existing results reported in the literature, even with much less data and considerably  
 357 simpler model/training procedure<sup>9</sup>. It is interesting that training on Movie dataset alone obtains

Table 2: Effect of color jitter ( $\sigma$ ) and computing contrastive loss in  $\ell_2$ -normalized embedding space with temperature hyper-parameter ( $\tau$ ) on different downstream tasks.

$k$	$\sigma$	HMDB51	ESC50	UCF101
1	0.0	60.32	86.50	85.69
16	0.0	62.92	88.33	86.30
1	1.0	60.45	87.66	84.82
16	0.5	60.13	87.75	85.98
16	1.0	61.11	88.33	85.93
$k$	$\tau$	HMDB51	ESC50	UCF101
16	0.07	60.78	87.08	86.86
16	0.30	60.78	89.25	85.72

Table 3: Effect of genre distribution in Movie dataset on different downstream tasks. Experiments are conducted with input spatial resolution of  $112 \times 112$  pixels.

setting	HMDB51	ESC50	UCF101
i	57.58	86.50	82.44
ii	56.99	85.50	82.39
iii	56.27	85.25	82.87
iv	56.40	86.75	83.24

<sup>8</sup>the data is not publicly available, and similarly the implementation to train XDC[3]

<sup>9</sup>supplemental material includes comparison of training costs



Table 5: Comparison with state-of-the-art. Dataset abbreviations: **AudioSet**[11], **HowTo100M**[28], **IG-Kinetics65M** [12]; their length in years is given in the “years” column. “Arch.” denotes the architecture of video backbone ( $f$ ). [2]<sup>†</sup> indicates when the corresponding model use only audio and video, and not text modality. For a fair comparison, when using only Movie dataset, we train for twice as many epochs as our other variants in order to match their total number of gradient updates.

Method	Arch.	pretraining dataset	curated	years	HMDB51	UCF101	ESC50
GDT[39]	R(2+1)D-18	AS	✓	1	66.1	92.5	88.5
GDT[39]	R(2+1)D-18	IG65M	✓	21	72.8	95.2	
XDC[3]	R(2+1)D-18	AS	✓	1	61.0	91.2	84.8
XDC[3]	R(2+1)D-18	IG65M	✓	21	67.4	94.2	
AVTS[22]	MC3	AS	✓	1	61.6	89.0	82.3
AVID[31]	R(2+1)D-18	AS	✓	1	64.7	91.5	89.1
MMV[2] <sup>†</sup>	R(2+1)D-18	AS	✓	1	70.1	91.5	85.6
MMV[2] <sup>†</sup>	S3D-G	AS	✓	1	68.2	90.1	86.1
MMV[2] <sup>†</sup>	S3D-G	AS+HT	✓	16	68.3	91.1	87.2
Ours ( $k=16$ )	R(2+1)D-18	Movie	✗	0.7	64.5	87.9	88.8
Ours ( $k=8$ )	R(2+1)D-18	Movie+TV	✗	1.4	65.0	87.7	89.1
Ours ( $k=16$ )	R(2+1)D-18	Movie+TV	✗	1.4	65.1	88.5	89.1
Ours ( $k=32$ )	R(2+1)D-18	Movie+TV	✗	1.4	65.6	88.7	88.2

358 comparable performance to the cases where both TV and Movie datasets are used for pretraining.  
 359 This further confirms the richness of the training data which movies and TV shows can provide  
 360 to self-supervised learning problems. We also see that increasing  $k$  even beyond 8 gives further  
 361 incremental gains on action recognition benchmarks.

## 362 5 Conclusion

363 Despite its amazing recent progress, state-of-the-art self-supervised learning still heavily relies on  
 364 supervised, *i.e.* curated, large-scale datasets for pretraining. In this work, we have shown that  
 365 pretraining solely on uncurated data in forms of movies and TV shows, even at a comparatively  
 366 small scale, can give rise to representations which are capable of competing with the state-of-the-  
 367 art of more complex architectures trained on larger curated datasets. This comes contrary to the  
 368 current literature which tends to suggest that learning from uncurated data largely falls behind  
 369 the use of curated alternatives. We intentionally made design decisions to keep our approach and  
 370 training strategy as simple as possible to demonstrate that learning decently powerful audio-visual  
 371 representations does not necessarily require gigantic data and compute resources. Through extensive  
 372 set of experiments, our work establishes for the first time the efficacy of self-supervised learning of  
 373 audio-visual representations from movies and TV shows.

## 374 6 Broader impact

375 **Potential benefits.** Our work shows that competitive multimodal representations can be learned  
 376 from a comparatively small volume of *uncurated* data in the form of movies and TV shows. Besides  
 377 minimizing any sort of human-involvement, which we believe must have already been paid an  
 378 extra attention to in the literature, our work demonstrates that one does not require gigantic data and  
 379 compute resources for effective self-supervised pretraining. Such results promise a more democratized  
 380 research arena where smaller groups are not alienated due lack of sufficient compute resources. More  
 381 importantly, lowering the compute requirements naturally reduces any environmental effects which  
 382 training these models can potentially have.

383 **Potential risks.** Any machine learning method is susceptible to the potential underlying biases in  
 384 the data. This is more important for self-supervised methods that deal with huge volumes, often not  
 385 evaluated by diverse group of humans for any fairness concerns. The same is generally true in our  
 386 case which requires us to make sure that titles that are included in training are diverse and inclusive.

387 **References**

- 388 [1] S. Abu-El-Haija, N. Kothari, J. Lee, P. Natsev, G. Toderici, B. Varadarajan, and S. Vijayanarasimhan.  
389 Youtube-8m: A large-scale video classification benchmark. *arXiv preprint arXiv:1609.08675*, 2016.
- 390 [2] J.-B. Alayrac, A. Recasens, R. Schneider, R. Arandjelović, J. Ramapuram, J. De Fauw, L. Smaira,  
391 S. Dieleman, and A. Zisserman. Self-Supervised MultiModal Versatile Networks. In *NeurIPS*, 2020.
- 392 [3] H. Alwassel, D. Mahajan, B. Korbar, L. Torresani, B. Ghanem, and D. Tran. Self-supervised learning by  
393 cross-modal audio-video clustering. In *Advances in Neural Information Processing Systems*, volume 33,  
394 pages 9758–9770, 2020.
- 395 [4] R. Arandjelovic and A. Zisserman. Look, listen and learn. In *Proceedings of the IEEE International  
396 Conference on Computer Vision*, pages 609–617, 2017.
- 397 [5] P. Bachman, R. D. Hjelm, and W. Buchwalter. Learning representations by maximizing mutual information  
398 across views. In *Advances in Neural Information Processing Systems*, pages 15535–15545, 2019.
- 399 [6] J. Carreira and A. Zisserman. Quo vadis, action recognition? a new model and the kinetics dataset. In  
400 *proceedings of the IEEE Conference on Computer Vision and Pattern Recognition*, pages 6299–6308,  
401 2017.
- 402 [7] T. Chen, S. Kornblith, M. Norouzi, and G. Hinton. A simple framework for contrastive learning of visual  
403 representations. *arXiv preprint arXiv:2002.05709*, 2020.
- 404 [8] T. Chen, S. Kornblith, K. Swersky, M. Norouzi, and G. Hinton. Big self-supervised models are strong  
405 semi-supervised learners. *arXiv preprint arXiv:2006.10029*, 2020.
- 406 [9] C. Doersch, A. Gupta, and A. A. Efros. Unsupervised visual representation learning by context prediction.  
407 In *Proceedings of the IEEE international conference on computer vision*, pages 1422–1430, 2015.
- 408 [10] B. Fernando, H. Bilen, E. Gavves, and S. Gould. Self-supervised video representation learning with  
409 odd-one-out networks. In *Proceedings of the IEEE conference on computer vision and pattern recognition*,  
410 pages 3636–3645, 2017.
- 411 [11] J. F. Gemmeke, D. P. Ellis, D. Freedman, A. Jansen, W. Lawrence, R. C. Moore, M. Plakal, and M. Ritter.  
412 Audio set: An ontology and human-labeled dataset for audio events. In *2017 IEEE International Conference  
413 on Acoustics, Speech and Signal Processing (ICASSP)*, pages 776–780. IEEE, 2017.
- 414 [12] D. Ghadiyaram, D. Tran, and D. Mahajan. Large-scale weakly-supervised pre-training for video action  
415 recognition. In *Proceedings of the IEEE Conference on Computer Vision and Pattern Recognition*, pages  
416 12046–12055, 2019.
- 417 [13] S. Gidaris, P. Singh, and N. Komodakis. Unsupervised representation learning by predicting image  
418 rotations. *arXiv preprint arXiv:1803.07728*, 2018.
- 419 [14] M. Gutmann and A. Hyvärinen. Noise-contrastive estimation: A new estimation principle for unnormalized  
420 statistical models. In *Proceedings of the Thirteenth International Conference on Artificial Intelligence and  
421 Statistics*, pages 297–304, 2010.
- 422 [15] K. He, H. Fan, Y. Wu, S. Xie, and R. Girshick. Momentum contrast for unsupervised visual representation  
423 learning. In *Proceedings of the IEEE/CVF Conference on Computer Vision and Pattern Recognition*, pages  
424 9729–9738, 2020.
- 425 [16] K. He, X. Zhang, S. Ren, and J. Sun. Deep residual learning for image recognition. In *Proceedings of the  
426 IEEE conference on computer vision and pattern recognition*, pages 770–778, 2016.
- 427 [17] O. J. Hénaff, A. Srinivas, J. De Fauw, A. Razavi, C. Doersch, S. Eslami, and A. v. d. Oord. Data-efficient  
428 image recognition with contrastive predictive coding. *arXiv preprint arXiv:1905.09272*, 2019.
- 429 [18] R. D. Hjelm, A. Fedorov, S. Lavoie-Marchildon, K. Grewal, P. Bachman, A. Trischler, and Y. Bengio.  
430 Learning deep representations by mutual information estimation and maximization. *arXiv preprint  
431 arXiv:1808.06670*, 2018.
- 432 [19] S. Ioffe and C. Szegedy. Batch normalization: Accelerating deep network training by reducing internal  
433 covariate shift. *arXiv preprint arXiv:1502.03167*, 2015.
- 434 [20] H. Kataoka, T. Wakamiya, K. Hara, and Y. Satoh. Would mega-scale datasets further enhance spatiotempo-  
435 ral 3d cnns? *arXiv preprint arXiv:2004.04968*, 2020.

- 436 [21] D. Kim, D. Cho, and I. S. Kweon. Self-supervised video representation learning with space-time cubic  
437 puzzles. In *Proceedings of the AAAI Conference on Artificial Intelligence*, volume 33, pages 8545–8552,  
438 2019.
- 439 [22] B. Korbar, D. Tran, and L. Torresani. Cooperative learning of audio and video models from self-supervised  
440 synchronization. In *Advances in Neural Information Processing Systems*, pages 7763–7774, 2018.
- 441 [23] H. Kuehne, H. Jhuang, E. Garrote, T. Poggio, and T. Serre. Hmdb: a large video database for human  
442 motion recognition. In *2011 International Conference on Computer Vision*, pages 2556–2563. IEEE, 2011.
- 443 [24] Z. Lai and W. Xie. Self-supervised learning for video correspondence flow. *arXiv preprint*  
444 *arXiv:1905.00875*, 2019.
- 445 [25] H.-Y. Lee, J.-B. Huang, M. Singh, and M.-H. Yang. Unsupervised representation learning by sorting  
446 sequences. In *Proceedings of the IEEE International Conference on Computer Vision*, pages 667–676,  
447 2017.
- 448 [26] D. Mahajan, R. Girshick, V. Ramanathan, K. He, M. Paluri, Y. Li, A. Bharambe, and L. van der Maaten.  
449 Exploring the limits of weakly supervised pretraining. In *Proceedings of the European Conference on*  
450 *Computer Vision (ECCV)*, pages 181–196, 2018.
- 451 [27] A. Miech, J.-B. Alayrac, L. Smaira, I. Laptev, J. Sivic, and A. Zisserman. End-to-end learning of visual  
452 representations from uncurated instructional videos. In *Proceedings of the IEEE/CVF Conference on*  
453 *Computer Vision and Pattern Recognition*, pages 9879–9889, 2020.
- 454 [28] A. Miech, D. Zhukov, J.-B. Alayrac, M. Tapaswi, I. Laptev, and J. Sivic. Howto100m: Learning a  
455 text-video embedding by watching hundred million narrated video clips. In *Proceedings of the IEEE*  
456 *international conference on computer vision*, pages 2630–2640, 2019.
- 457 [29] I. Misra and L. v. d. Maaten. Self-supervised learning of pretext-invariant representations. In *Proceedings*  
458 *of the IEEE/CVF Conference on Computer Vision and Pattern Recognition*, pages 6707–6717, 2020.
- 459 [30] I. Misra, C. L. Zitnick, and M. Hebert. Shuffle and learn: unsupervised learning using temporal order  
460 verification. In *European Conference on Computer Vision*, pages 527–544. Springer, 2016.
- 461 [31] P. Morgado, N. Vasconcelos, and I. Misra. Audio-visual instance discrimination with cross-modal  
462 agreement. *arXiv preprint arXiv:2004.12943*, 2020.
- 463 [32] V. Nair and G. E. Hinton. Rectified linear units improve restricted boltzmann machines. In *ICML*, 2010.
- 464 [33] M. Noroozi and P. Favaro. Unsupervised learning of visual representations by solving jigsaw puzzles. In  
465 *European Conference on Computer Vision*, pages 69–84. Springer, 2016.
- 466 [34] M. Noroozi, H. Pirsiavash, and P. Favaro. Representation learning by learning to count. In *Proceedings of*  
467 *the IEEE International Conference on Computer Vision*, pages 5898–5906, 2017.
- 468 [35] A. v. d. Oord, Y. Li, and O. Vinyals. Representation learning with contrastive predictive coding. *arXiv*  
469 *preprint arXiv:1807.03748*, 2018.
- 470 [36] A. Owens and A. A. Efros. Audio-visual scene analysis with self-supervised multisensory features. In  
471 *Proceedings of the European Conference on Computer Vision (ECCV)*, pages 631–648, 2018.
- 472 [37] A. Owens, J. Wu, J. H. McDermott, W. T. Freeman, and A. Torralba. Ambient sound provides supervision  
473 for visual learning. In *European conference on computer vision*, pages 801–816. Springer, 2016.
- 474 [38] D. Pathak, P. Krahenbuhl, J. Donahue, T. Darrell, and A. A. Efros. Context encoders: Feature learning  
475 by inpainting. In *Proceedings of the IEEE conference on computer vision and pattern recognition*, pages  
476 2536–2544, 2016.
- 477 [39] M. Patrick, Y. M. Asano, R. Fong, J. F. Henriques, G. Zweig, and A. Vedaldi. Multi-modal self-supervision  
478 from generalized data transformations. *arXiv preprint arXiv:2003.04298*, 2020.
- 479 [40] K. J. Piczak. Esc: Dataset for environmental sound classification. In *Proceedings of the 23rd ACM*  
480 *international conference on Multimedia*, pages 1015–1018, 2015.
- 481 [41] S. Purushwalkam and A. Gupta. Demystifying contrastive self-supervised learning: Invariances, augmen-  
482 tations and dataset biases. In H. Larochelle, M. Ranzato, R. Hadsell, M. F. Balcan, and H. Lin, editors,  
483 *Advances in Neural Information Processing Systems*, volume 33, pages 3407–3418, 2020.

- 484 [42] K. Soomro, A. R. Zamir, and M. Shah. Ucf101: A dataset of 101 human actions classes from videos in the  
485 wild. *arXiv preprint arXiv:1212.0402*, 2012.
- 486 [43] C. Sun, A. Shrivastava, S. Singh, and A. Gupta. Revisiting unreasonable effectiveness of data in deep  
487 learning era. In *Proceedings of the IEEE international conference on computer vision*, pages 843–852,  
488 2017.
- 489 [44] Y. Tian, D. Krishnan, and P. Isola. Contrastive multiview coding. *arXiv preprint arXiv:1906.05849*, 2019.
- 490 [45] D. Tran, H. Wang, L. Torresani, J. Ray, Y. LeCun, and M. Paluri. A closer look at spatiotemporal  
491 convolutions for action recognition. In *Proceedings of the IEEE conference on Computer Vision and  
492 Pattern Recognition*, pages 6450–6459, 2018.
- 493 [46] C. Vondrick, A. Shrivastava, A. Fathi, S. Guadarrama, and K. Murphy. Tracking emerges by colorizing  
494 videos. In *Proceedings of the European conference on computer vision (ECCV)*, pages 391–408, 2018.
- 495 [47] F. Wang and H. Liu. Understanding the behaviour of contrastive loss. *arXiv preprint arXiv:2012.09740*,  
496 2020.
- 497 [48] J. Wang, J. Jiao, L. Bao, S. He, Y. Liu, and W. Liu. Self-supervised spatio-temporal representation learning  
498 for videos by predicting motion and appearance statistics. In *Proceedings of the IEEE Conference on  
499 Computer Vision and Pattern Recognition*, pages 4006–4015, 2019.
- 500 [49] D. Xu, J. Xiao, Z. Zhao, J. Shao, D. Xie, and Y. Zhuang. Self-supervised spatiotemporal learning via video  
501 clip order prediction. In *Proceedings of the IEEE Conference on Computer Vision and Pattern Recognition*,  
502 pages 10334–10343, 2019.
- 503 [50] R. Zhang, P. Isola, and A. A. Efros. Colorful image colorization. In *European conference on computer  
504 vision*, pages 649–666. Springer, 2016.

## 505 Checklist

- 506 1. For all authors...
- 507 (a) Do the main claims made in the abstract and introduction accurately reflect the paper’s  
508 contributions and scope? [Yes]
- 509 (b) Did you describe the limitations of your work? [Yes] Specifically, training data  
510 being proprietary creates concerns around reproducibility, which has precedence in the  
511 literature as mentioned in the paper. We address that partially by planning to publicly  
512 release pretrained models.
- 513 (c) Did you discuss any potential negative societal impacts of your work? [Yes]
- 514 (d) Have you read the ethics review guidelines and ensured that your paper conforms to  
515 them? [Yes]
- 516 2. If you are including theoretical results...
- 517 (a) Did you state the full set of assumptions of all theoretical results? [N/A]
- 518 (b) Did you include complete proofs of all theoretical results? [N/A]
- 519 3. If you ran experiments...
- 520 (a) Did you include the code, data, and instructions needed to reproduce the main exper-  
521 imental results (either in the supplemental material or as a URL)? [No] The data is  
522 proprietary. However, we have provided implementation of the proposed method in  
523 supplemental material and aim to publicly release the pretrained models.
- 524 (b) Did you specify all the training details (e.g., data splits, hyperparameters, how they  
525 were chosen)? [Yes] They are all discussed in detail either in the main submission or in  
526 supplemental material.
- 527 (c) Did you report error bars (e.g., with respect to the random seed after running experi-  
528 ments multiple times)? [Yes] We only observed meaningful differences after running  
529 experiments multiple times, for ESC50[40] downstream experiments. Corresponding  
530 standard errors are reported in supplemental material.
- 531 (d) Did you include the total amount of compute and the type of resources used (e.g., type  
532 of GPUs, internal cluster, or cloud provider)? [Yes] Please refer to Section 4.1.

- 533 4. If you are using existing assets (e.g., code, data, models) or curating/releasing new assets...
- 534 (a) If your work uses existing assets, did you cite the creators? [N/A]
- 535 (b) Did you mention the license of the assets? [N/A]
- 536 (c) Did you include any new assets either in the supplemental material or as a URL? [N/A]
- 537
- 538 (d) Did you discuss whether and how consent was obtained from people whose data you're
- 539 using/curating? [N/A]
- 540 (e) Did you discuss whether the data you are using/curating contains personally identifiable
- 541 information or offensive content? [N/A]
- 542 5. If you used crowdsourcing or conducted research with human subjects...
- 543 (a) Did you include the full text of instructions given to participants and screenshots, if
- 544 applicable? [N/A]
- 545 (b) Did you describe any potential participant risks, with links to Institutional Review
- 546 Board (IRB) approvals, if applicable? [N/A]
- 547 (c) Did you include the estimated hourly wage paid to participants and the total amount
- 548 spent on participant compensation? [N/A]